

## **VEHICLE MATHEMATICAL MODEL FOR THE STUDY OF CORNERING**

**Preda Ion, Ciolan Gheorghe**

Transilvania University of Braşov

pion@unitbv.ro

**Keywords:** vehicle cornering, steering system, mathematical model, computer simulation.

**Abstract:** The aim of this work was to give theoretical tools for the study of vehicle cornering and handling. Starting for a simplified tire model, two dynamic and mathematical models were imagined for the vehicle, both able to include influences of steering, traction and braking systems. The models can be easily adapted for different vehicle types. The programs Matlab-Simulink and PTC MathCAD were chosen to solve the models equations. The computer simulations performed were used to determine the vehicle cornering behavior in various driving conditions.

### **1. INTRODUCTION**

Cornering and handling qualities of a motor vehicle constitute important aspects of the active safety, directly related with the dynamic performances and traffic safety. Consequently, even for the design stage, knowing the handling characteristics and controlling the means that can influence them have very big importance for the automotive engineers. Computer simulation permits to obtain useful information about cornering and handling, rapidly and at low costs.

The aim of this work was to find improvement possibilities for the car handling performances. For this purpose, two dynamic and mathematic vehicle models were imagined: one considering all the vehicle wheels and a simplified one, an extension of the basic "bicycle" model. Both dynamic models are planar (with three degrees of freedom for the vehicle body), but are able to include new influences for steering, traction and braking systems. The models can be easily adapted for other vehicles types. The programs Matlab-Simulink and PTC Mathcad were chosen to solve the model's equations. The computer simulations performed were used to determine the cornering and handling behavior of some cars in various conditions: driving maneuvers and post-collision displacement.

Experimental data, achieved in real conditions tests, was used to validate the models. The combination between theoretical and experimental investigations allows identifying modalities for car cornering and handling improvement. The results of this research can be useful for a better understanding of the automotive dynamics.

### **2. MODEL OF TIRE**

The key elements in the vehicle dynamics are the tires. Three physical processes contribute to the generation of the wheel-ground interaction force [1], [2], better known as the **grip force**:

- **adhesion**, that arises (in the dimensional range of 1 nm to 1  $\mu$ m) from the intermolecular bonds between the rubber and the aggregate in the ground surface, producing shear stresses;
- **hysteresis** (indentation), that means the appearance of a force in the contact patch due to the supplementary energy loss in the rubber as it deforms to cover

the road irregularities (in the range of 10 μm to 1 mm) when a (driving or braking) torque or a lateral force are applied to the tire or when the wheel is steered (changing its orientation with respect to its displacement direction);

- **soil resistance to distortion**, that produces (in the macro dimensional range) only when the ribs of the wheel engage the soft (deformable) ground or the hard ground's large irregularities.

To generate tire-ground grip force, two elements must exist:

- **normal load**, a force that presses the tire against the ground;
- **tire slip** (or at least a tendency to slip).

If one of these two is missing, no friction force will be generated.

Practically, the friction force can reach in any direction almost the same maximal absolute value [4], named the **peak friction force**, which can be computed with the equation

$$F_{\max} = \mu_P Z \tag{1}$$

where  $Z$  is the normal load of the tire and  $\mu_P$  is the **peak friction coefficient** that indicate the best grip properties in a given tire-ground interface. The change of the grip force due to the camber can be considered modifying the value of  $\mu_P$ .

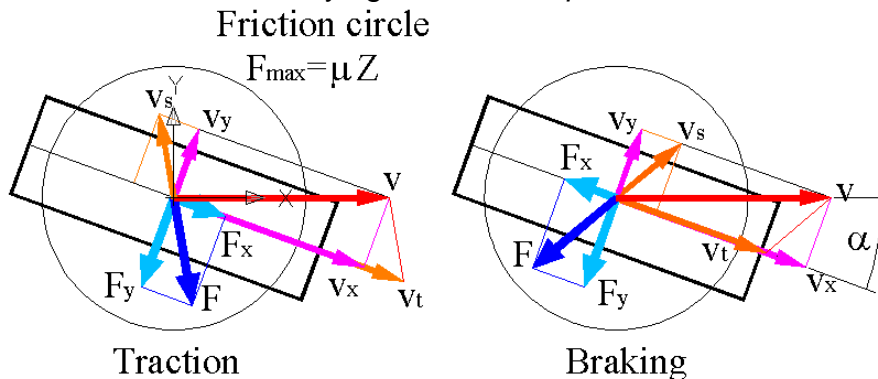


**Figure 1. Velocities and friction forces in the tire-ground contact patch (upper view, right turn)**

For most of the driving condition, it can be considered the grip force is acting on the center of the tire-ground contact patch. The grip force has the same support as the tire's sliding speed (with respect to the ground) but an opposite orientation [3].

It considers a mobile coordinate system  $x_w C_{cp} y_w$  attached to the centre of wheel contact patch and having the semi-axis  $x_w$  pointing forward in the wheel's centre plane (longitudinal plane), **figure 1**. During movement, the tire's point in the centre of contact patch has the **theoretical velocity** (rolling velocity)  $v_t = \Omega r_d$  (with  $\Omega$  the rotating speed of the wheel and  $r_d$  the dynamic radius of the wheel), that has as support the semi-axis  $x_w$ . The wheel's **real velocity**  $v$  makes with the vector  $v_t$  (and semi-axis  $x_w$ ) the **slip angle**  $\alpha$ . The vectorial difference  $\vec{v}_s = \vec{v} - \vec{v}_t$  represents the **slip velocity** that the wheel slides on the ground. The real velocity and the slip velocity can be also considered as resultant of their components:

$$\vec{v} = \vec{v}_t + \vec{v}_s = \vec{v}_x + \vec{v}_y, \quad \vec{v}_s = \vec{v}_{sx} + \vec{v}_{sy} \tag{2}$$

The **actual friction force**  $\vec{F}$  acting on tire has the same support as the slip

velocity vector, but opposite orientation (the force opposes to the slip). Its magnitude depends on the peak friction force and on the tire's **total slip**  $s$ , defined as

$$s = v_s / v_x = \sqrt{\kappa^2 + tg^2\alpha} \quad (3)$$

The components of the total slip are the longitudinal slip  $\kappa$ :

$$\kappa = v_{sx} / v_x = \begin{cases} 1 - \frac{v_x}{v_t} & \text{if } v_x < v_t \\ 0 & \text{if } v_x = v_t \\ -\left(1 - \frac{v_t}{v_x}\right) & \text{if } v_x > v_t \end{cases} \quad (4)$$

and the lateral slip

$$tg\alpha = v_{sy} / v_x \quad (5)$$

with  $\alpha$  the slip angle.

The **figure 2** shows a typical representation of the **relative friction coefficient** (indicating the fraction of  $F_{max}$  that is generated in the contact patch)

$$\xi = F / F_{max} \quad (6)$$

as a function of total slip  $s$  (with values limited between -1 and 1). In the ISO convention, it considers positive values for  $s$  and  $\xi$  during traction and negative values for braking.

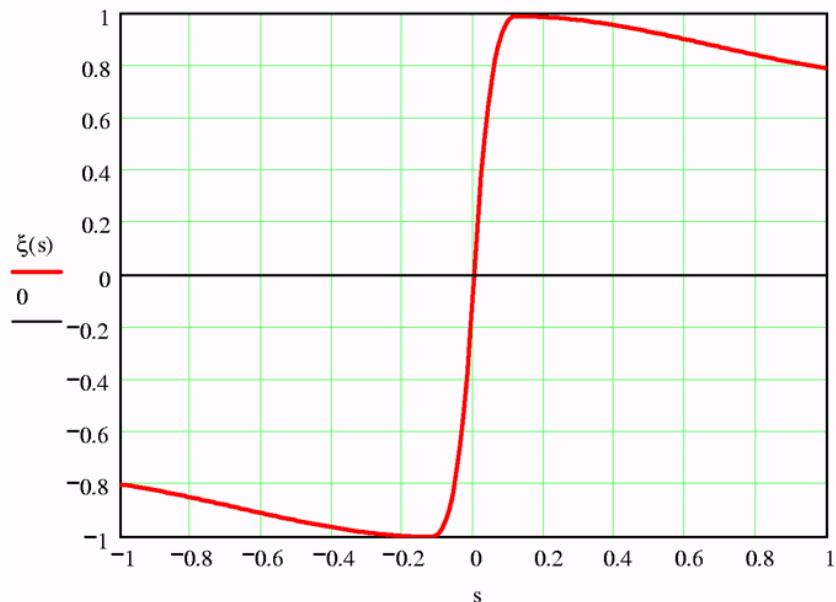


**Figure 2. Tire's actual friction coefficient vs. total slip**

The (actual) **friction coefficient**  $\mu$  (also called "used friction") and the tire's (actual) friction force  $F$  are

$$\mu = \mu_P \xi \quad F = \mu Z = \mu_P \xi Z = \xi F_{max} \quad (7)$$

The curve  $\xi(s)$  has two important domains for both traction and braking:

- the domain of **small slip**, also named pseudo-slip ( $s < 0.05 \dots 0.1$ ), characterized by the absence of slide in the contact patch; the appearance of slip come from the tire material's elastic deformation under stress;
- the domain of **evident slip**, characterized by the existence of slide in the contact patch, phenomenon evidenced by black tire marks on hard grounds; if  $|s|=1$ , the slide appears in any point of the contact patch ( $s=1$  means the wheel spins, but no wheel translation produces;  $s=-1$  means the wheel is locked, but continue to translate); when slide occurs only in a small area of the contact patch (normally, in the field  $0.1 < |s| < 0.3$ ), the absolute friction force takes the biggest values.

To mathematically model the shape of  $\xi(s)$  curve, many formulae, more or less empirical, were suggested [4]. Anyway, this shape is defined well enough by only some quantities:

- the slope at the origin, proportional to the tire stiffness;
- the slip value  $s_P$  that corresponds to the maximal grip ( $\mu_P, F_{\max}$ );
- the value of the friction coefficient  $\mu_S$  that corresponds to the total slip ( $s=1$  or  $s=-1$ ) and the slope of the curve in the area of total slip.

### 3. FOUR-WHEEL MODEL OF THE FULL VEHICLE

The friction forces of all the wheels and the grade and aerodynamic resistances produce continuous variations of the dynamic load  $Z$  of each wheel [1], [2], [5], [9]. The computation of these loads can be performed using quasi-static or dynamic suspension models that include pitch and roll degrees of freedom. If desired, even the change of the wheel's dynamic radius  $r_d$  under variable load can be also considered [5].

To control the friction force of the tire, two possibilities exist:

- to modify the longitudinal slip  $\kappa$  by the application of a driving or braking torque that accelerates or brakes the wheel spinning and implicitly change the theoretical velocity  $v_t$ ;
- to modify the lateral slip  $\text{tg}\alpha$  by steering the wheel, i.e. changing its position relative to the real velocity  $v$  (the angle  $\alpha$ ).

To compute the friction force of a certain wheel it is necessary to know the dynamic load, the peak friction coefficient and the orientation and magnitude of two vectors: real and theoretical velocities.

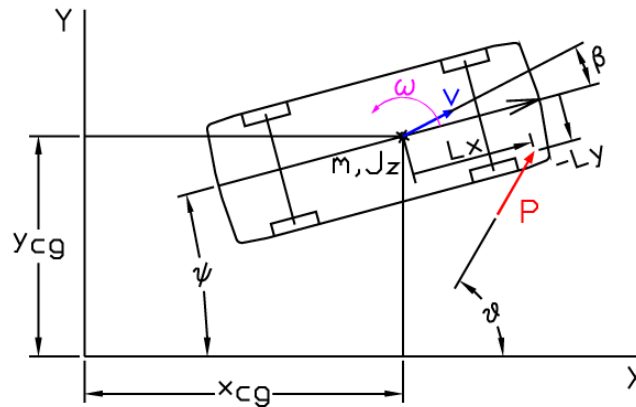


**Figure 3. Planar model of the vehicle**

The real velocity of a contact patch centre computes adding the velocity associated to the yaw speed to the velocity  $\vec{v}_{cg}$  of the vehicle's centre of gravity (**figure 3**):

$$\vec{v} = \vec{v}_{cg} + \vec{\omega} \vec{d}_w \quad (8)$$

where  $\vec{d}_w$  represents the distance vector between the centre of gravity and the middle of the contact patch.

To compute the other velocity, the theoretical one, it is necessary to simulate the functioning of the driving and braking systems [5] or to make some assumptions about the longitudinal slip  $\kappa$  or about the magnitude of the longitudinal force  $F_x$ .

Important simplifications can be made if one considers two extreme cases. The first one corresponds to a **free wheel** (no torque is applied). In this situation, the friction coefficient is equal with the rolling resistance coefficient,  $\xi = -f$  and the longitudinal slip  $\kappa$  is very small and can be neglected.

The second case considers a **locked wheel**, under the effect of a panic braking. This means  $\kappa = -1$  and  $\xi = -\mu_S$ , the value that corresponds to the total slip.

Accordingly with **figure 1** and **figure 3**, the wheel slip angle  $\alpha_w$  it is computed with the equation:

$$\alpha_w = \arctg\left(\frac{v_{wy}}{v_{wx}}\right) - (\psi + \delta_w) \quad (9)$$

as function of the longitudinal and transversal components ( $v_{wx}$ ,  $v_{wy}$ ) of the real velocity, the actual heading angle  $\psi$  and the wheel steering angle  $\delta_w$ .

Now, with the equations (2)...(5) can be determined the vector  $\vec{v}_s$ , then the orientation and the magnitude of the friction force  $F = f(\mu_P, \xi, Z)$  and finally its components in tangential and lateral direction

$$F_x = \frac{\kappa}{\sqrt{\kappa^2 + tg^2 \alpha}} F_{max} \quad F_y = \frac{tg \alpha}{\sqrt{\kappa^2 + tg^2 \alpha}} F_{max} \quad (10)$$

Further, using the forces of all the wheels, it is possible to write the system of three equations that defines the vehicle's dynamic behavior (in the fixed coordinate system):

$$\begin{aligned}
 a_X &= \frac{\Sigma(X_W \cdot \cos(\psi + \delta_W) - Y_W \cdot \sin(\psi + \delta_W))}{m} \\
 a_Y &= \frac{\Sigma(X_W \cdot \sin(\psi + \delta_W) + Y_W \cdot \cos(\psi + \delta_W))}{m} \\
 \varepsilon_Z &= \frac{(Y_{fl} \cdot \cos(\delta_{fl}) + X_{fl} \cdot \sin(\delta_{fl}) + Y_{fr} \cdot \cos(\delta_{fr}) + X_{fr} \cdot \sin(\delta_{fr})) \cdot L_a}{J_z} \dots \\
 &+ \frac{(-Y_{rl} \cdot \cos(\delta_{rl}) - X_{rl} \cdot \sin(\delta_{rl}) - Y_{rr} \cdot \cos(\delta_{rr}) - X_{rr} \cdot \sin(\delta_{rr})) \cdot L_b}{J_z} \dots \\
 &+ \frac{(Y_{fl} \cdot \sin(\delta_{fl}) - X_{fl} \cdot \cos(\delta_{fl}) + Y_{rl} \cdot \sin(\delta_{rl}) - X_{rl} \cdot \cos(\delta_{rl})) \cdot \frac{E}{2}}{J_z} \dots \\
 &+ \frac{(-Y_{fr} \cdot \sin(\delta_{fr}) + X_{fr} \cdot \cos(\delta_{fr}) - Y_{rr} \cdot \sin(\delta_{rr}) + X_{rr} \cdot \cos(\delta_{rr})) \cdot \frac{E}{2}}{J_z} \dots
 \end{aligned} \tag{11}$$

Then, integrating numerically these equations, it obtains the velocities ( $v_x, v_y, \omega$ ) and the displacements ( $s_x, s_y, \psi$ ) of the vehicle's centre of gravity.

#### 4. TWO-WHEEL MODEL OF THE FULL VEHICLE

The dynamic model presented here – an extension of the so called “bicycle” model – is able to describe the basic cornering behavior in various traveling conditions of a two-axle vehicle and can include other influences for steering, traction and braking systems. It can lead to a better understanding of the motor vehicle dynamics.

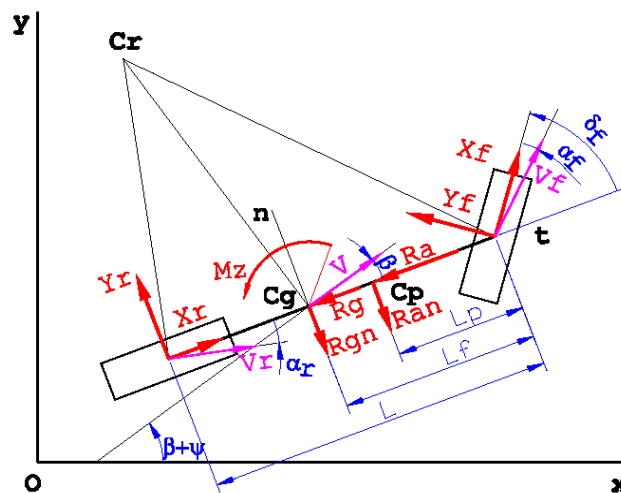


**Figure 4. “Bicycle” model for vehicle’s cornering dynamics**

Normally, experimental data, achieved in real conditions tests, is necessary first to calibrate the model (to realize fine adjustment of the model parameters) and to validate the model (to confirm the correctness of the results).

The vehicle’s planar dynamic-model presented in **figure 4** is called “single-track” or “bicycle” model. Its main characteristic is the replacement of the both wheels of an axle with only one wheel that has equivalent kinematic and dynamic behavior. The model will not consider explicitly the effects of roll movement and camber change, but can be relatively easy adapted to take account of these phenomena.

It considers that the vehicle moves on a planar curved trajectory, with its instantaneous centre of rotation  $C_r$  determined by the speed vectors  $\vec{v}_f$  and  $\vec{v}_s$  of front and rear axles. The speed vector  $\vec{v}$  corresponds to the centre of gravity  $C_g$ , which generally

adopts as the control point (the control point of a vehicle is a point whose current position and trajectory presents maximal interest for the driving process).

Two coordinate systems are considered: one fixed and the other mobile. The fixed system  $xOy$  is attached to the ground (non-dependent by the vehicle positions). The mobile system  $tC_gn$  is linked to the vehicle. This has the origin in the vehicle's centre of gravity  $C_g$ , its axis  $t$  is the vehicle's longitudinal axis and the transversal axis  $n$  is perpendicular to the axis  $t$ .

The aerodynamic force is the resultant of the components  $R_a$  and  $R_{an}$ , which act on the two directions and focus in the centre of pressure  $C_p$ .

The influence of road declivity is taken into consideration by the forces  $R_g$  and  $R_{gn}$ , both acting in the centre of gravity. The force  $R_g$ , disposed on the longitudinal axis of the car, represents the grade resistance; the force  $R_{gn}$ , acting on the  $n$  direction, is a consequence of the road declivity in the vehicle's transversal direction.

In the tire-road contact surfaces of the front and rear wheels act the tangential forces  $X_f$  and  $X_r$ , the lateral forces  $Y_f$  and  $Y_r$ , and the normal forces to the path  $Z_f$  and  $Z_r$ .

To consider the load transfer between the wheels on inner and outer sides of the turn or between the axles during traction or braking it is necessary to use supplementary models that include the behavior of the suspension.

The speed vector  $\vec{v}$  of the centre of gravity makes with the longitudinal axis  $t$  the angle  $\beta$ , named **sideslip angle** and indicating the lateral deviation of the vehicle. The speed  $\vec{v}$  can be decomposed in two perpendicular components:

$$\begin{aligned} v_t &= v \cos \beta \\ v_n &= v \sin \beta \end{aligned} \tag{12}$$

contained respectively in the vehicle's longitudinal and transversal planes.

As consequence of the translational and angular velocities ( $v$  and  $\omega$ ), in the centre of gravity will act:

- the tangential acceleration (on the velocity direction)

$$a_v = \frac{dv}{dt}; \tag{13}$$

- the centripetal acceleration (on the direction  $C_gC_r$ , the turning radius)

$$a_{cp} = v(\dot{\beta} + \dot{\Psi}) = v(\dot{\beta} + \omega) = v^2/R; \tag{14}$$

- the yaw acceleration

$$\varepsilon = \frac{d\omega}{dt} = \dot{\omega} = \ddot{\Psi}. \tag{15}$$

Decomposing the translational accelerations  $a_v$  and  $a_{cp}$  on the directions  $t$  and  $n$ , it obtain the expressions for the acceleration's longitudinal and transversal components in the centre of gravity:

$$\begin{aligned} a_t &= a_v \cos \beta - a_{cp} \sin \beta \\ a_n &= a_v \sin \beta + a_{cp} \cos \beta \end{aligned} \tag{16}$$

In the hypothesis of a non-violent cornering (with the transversal acceleration  $a_n$  smaller as  $4 \text{ m/s}^2$ ), it can consider that the tires' lateral forces are proportional to the corresponding slip angles:

$$Y_f = C_f \alpha_f \qquad Y_r = C_r \alpha_r. \qquad (17)$$

Combining relations (13)...(17), it can be written the system of three differential-equations (translations on directions  $t$  and  $n$  and yaw) that describes the vehicle behavior in any cornering situations, including transitory state:

$$\begin{aligned} \dot{v} \cos \beta - v (\dot{\beta} + \dot{\psi}) \sin \beta &= \frac{\sum F_t}{m} \\ \dot{v} \sin \beta - v (\dot{\beta} + \dot{\psi}) \cos \beta &= \frac{\sum F_n}{m} . \\ \ddot{\psi} &= \frac{\sum M_z}{J_z} \end{aligned} \qquad (18)$$

The three unknowns (the speed  $v$ , the slip angle  $\beta$  and the yaw angle  $\psi$ ) can be determined approximately by computer numerical integration only if there are known their initial values, the temporal evolutions of forces and yawing moment and the vehicle inertial characteristics ( $m$  – the vehicle's mass;  $J_z$  – the vehicle's moment of inertia about z axis).

The resultants of exterior forces and torques that appear in the previous system of equations are computed using the projections on the directions  $t$  and  $n$  of the gravitational, aerodynamic and tires forces. To calculate the longitudinal and lateral forces on tires it is necessary to consider the road grip characteristics and the driving and braking torques produced by the drivetrain and brakes.

If one considers small sideslip angle  $\beta$  ( $\sin \beta \approx \tan \beta \approx \beta$  and  $\cos \beta \approx 1$ ), then the system of equations (18) become:

$$\begin{aligned} \dot{v} - v (\dot{\beta} + \dot{\psi}) \beta &= \frac{\sum F_t}{m} \\ \dot{v} \beta - v (\dot{\beta} + \dot{\psi}) &= \frac{\sum F_n}{m} . \\ \ddot{\psi} &= \frac{\sum M_z}{J_z} \end{aligned} \qquad (19)$$

The first equation shows that if the sum of the longitudinal forces remains constant during cornering, the vehicle velocity will decrease to a lower level as before turning, or, in other words, when one negotiates a turn it is necessary to push more the accelerator pedal to maintain the same speed.

The equations for the steady-state cornering are obtained if ones consider constant sideslip angle ( $\beta$  constant;  $\dot{\beta} = 0$ ) and null values for translational and yaw accelerations:  $\dot{v} = 0$  ( $v$  constant) and  $\ddot{\psi} = 0$  ( $\dot{\psi} = \omega$  constant).



$$\begin{aligned}
 -v\dot{\psi}\beta &= \frac{\Sigma F_t}{m} & v\omega\beta &= -\frac{\Sigma F_t}{m} \\
 -v\dot{\psi} &= \frac{\Sigma F_n}{m} & \text{or} & & v\omega &= \frac{v^2}{R} = \omega^2 R = -\frac{\Sigma F_n}{m} \\
 0 &= \frac{\Sigma M_z}{J_z} & & & \Sigma M_z &= 0
 \end{aligned}
 \tag{20}$$

The third equation shows that during steady-state cornering the sum of the moments over the z axis in the centre of gravity must be null. That means the tires of the nearest axle to the centre of gravity must generate bigger lateral force and, as consequence, will experience bigger sideslip angle.

### 5. SIMULATION RESULTS

Based on the presented algorithms, computer programs were realized that permits to graphically represent different vehicles in their computed successive positions. For that, a database with bi- or tri-dimensional CAD models (**figure 5**) was designed and is continuously increasing by adding new models.

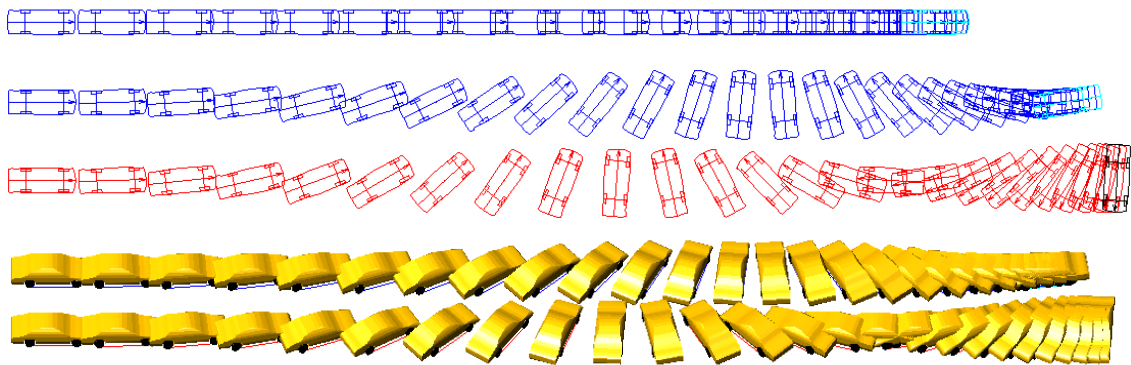


**Figure 5. Simulation of braking with locked wheels: up – homogenous surface ( $\mu=0.8$ ) middle –  $\mu$ -split condition ( $\mu_{hi}=0.8, \mu_{lo}=0.45$ ); bottom –  $\mu$ -split condition ( $\mu_{hi}=0.8, \mu_{lo}=0.1$ )**

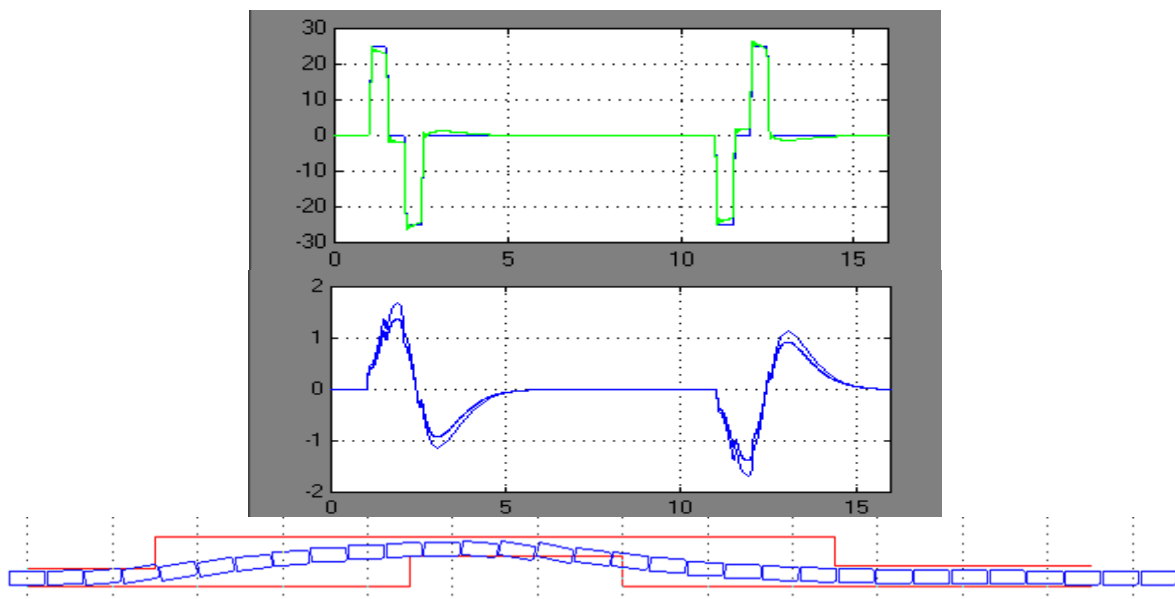


**Figure 6. Simulation results of an obstacle avoidance maneuver**

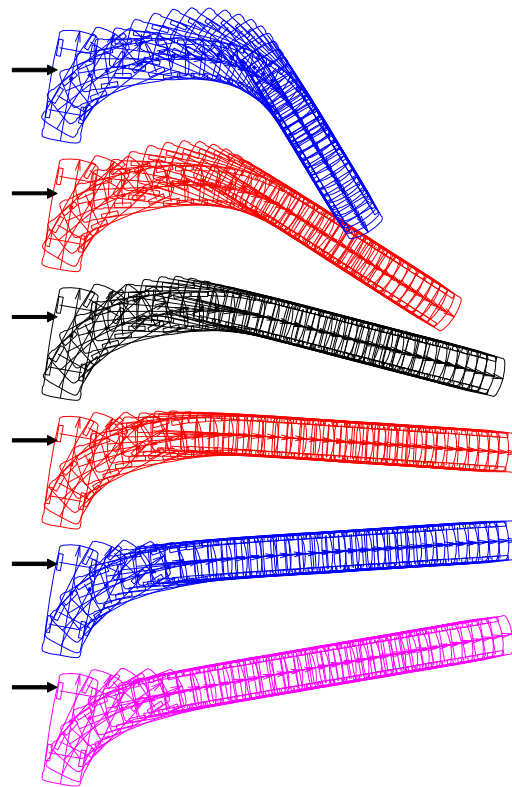


**Figure 7. Influence of the impact point on the post-impact trajectory and heading**

The program permits to assign different frictional properties for different areas of the ground, including gradual transitions for a value to other.

As an example of algorithm and graphic program possibilities, in **figure 5** it is presented the case of a car that brakes from 108 km/h with all the wheels locked. No steering angle is applied to the front wheels before and during braking. Three situations were considered: a homogenous road surface ( $\mu=0.8$ ) and two  $\mu$ -split conditions, with the same higher friction coefficient  $\mu_{hi}=0.8$  (on the left side), but different lower values:  $\mu_{lo}=0.45$ , respectively  $\mu_{lo}=0.1$ . The **figure 5** shows plots with successive vehicle positions computed at equal time interval of 0.2 s. The total stopping time, distance and yawing angle for these three situations are: 3.8 s, 57.4 m, vehicle maintains its initial orientation; 4.2 s, 66 m, 186°; 4.3 s, 69.8 m, 268°.

One of the most used maneuvers to appreciate the handling ability of a car is the double lane change that corresponds to overtake or obstacle avoidance [6], [8]. **Figure 6** shows such an example. The upper plot presents, versus time (s), the steering angles (deg) of the driver wheel (blue) and of the front wheels (green) – in this case, the simulation took into account the compliances of the steering shaft and linkage. The middle plot presents the lateral acceleration ( $m/s^2$ ) versus time (s) – the two plots correspond to the driver's steering input presented previously (25° max. angle) and to a weaker input (20° max. angle). The lower plot shows the vehicle's successive positions at equal time intervals (in this example, with the presented driver action on the steering wheel, the avoidance maneuver fails).

The last example is presented in **figure 7** and shows the possibility to use the algorithms for car accident reconstruction [7]. A stationary vehicle, with free wheels (the transmission on neutral and the brakes not applied) is impacted by another vehicle. The direction and the positions of the impact are indicated by the arrows. As the position and magnitude of the percussion changes, the trajectories of the impacted vehicle change

accordingly. The program permits also to compute and plot the trajectories of all the wheels and the values of their slip angles. Comparing the aspect of these trajectories (corresponding to large slip angles, able to remove rubber from the tires) with the tire marks observed at the accident scene, it is possible to estimate the direction and magnitude of the impact.

## **6. CONCLUSIONS**

The algorithms concisely presented in this article permits to simulate the car behavior in different driving situations (velocities, trajectories, running resistances, propulsion or braking forces) and to determine the influences of the constructive parameters, used as defining values of the mathematic model (cornering stiffness of the tires, position of the centre of gravity, position of the centre of pressure, characteristics of the steering system etc). The calculation permit to obtain the temporal evolutions for different interest quantities: forces and torques, linear or rotational accelerations, velocities and displacements.

The developed research method gives the possibility to simulate processes difficult to be investigated experimentally and can help to setup the main design characteristics of the entire car and of its steering system, starting early, in the conception phase. For improved results, the mathematical models can be tuned using experimental data.

### **References:**

- [1] Gillespie, T. *Fundamentals of Vehicle Dynamics*. SAE, Warrendale, USA, 1992.
- [2] Mitschke M., Wallentowitz H. *Dynamic der Kraftfahrzeuge (Motor Vehicle Dynamics)*. Springer-Verlag, 2004.
- [3] Pacejka H., Bakker E. *The Magic Formula Tyre Model*. *Vehicle System Dynamics*, Vol. 21, pp.1-18, 1991.
- [4] Preda I., Ciolan Gh. *Modelarea interacțiunii dintre roată și sol (Modelling of the Wheel-Ground Interaction)*. The VII<sup>th</sup> Automotive Conference "CAR '97", vol. A, pp.85-90, Pitești.
- [5] Preda I., Ciolan Gh., Dogariu M., Todor I. *Computer Model to Simulate the Vehicle Longitudinal Dynamics*. The X<sup>th</sup> International Automotive Congress "CONAT 2004", paper 1060, Brașov. ISBN 973-635-394-X
- [6] Preda, I., Vulpe, V., Enache, V. *Simulation of Driver Behaviour in Cornering Manoeuvre*. The X<sup>th</sup> International Automotive Congress "CONAT 2004", paper 1070, Brașov. ISBN 973-635-394-X
- [7] Preda I., Ciolan Gh., Covaciu D., Seitz N., Dima D.S. *Contributions to the Study of Vehicle Impact and Post-Impact Dynamics*. The IX<sup>th</sup> International Automotive Conference CAR 2005, paper 1082, Pitești.
- [8] Preda I., Enache V., Ciolan Gh. *Simularea asistată de calculator a maniabilității autoturismelor (Computer Based Simulation of Car Handling)*. International Conference "Sisteme de Transport și Logistică", pp.69-77, Ed. Evrica, Chișinău, 2005.
- [9] Preda I., Covaciu D., Ciolan Gh. *Coast-Down Test – Theoretical and Experimental Approach (Chapter Nineteen)*. In: "The Automobile and the Environment", pp. 277-288, Cambridge Scholars Publishing, Newcastle upon Tyne, 2011.